Supplementary data file

Selective fluorescence turn-on detection of combination cisplatin-etoposide chemotherapy based on N-CDs/GSH-CuNCs nanoprobe

Khalid Alhazzani[a], Ahmed Z. Alanazi[a], Aya M. Mostafa[b,c], James Barker[b], Mohamed M. El-Wekil[c], Al-Montaser Bellah H. Ali[c*]

[a] Department of Pharmacology and Toxicology, College of Pharmacy, King Saud University, Riyadh, Saudi Arabia.

[b] School of Life Sciences, Pharmacy, and Chemistry, Kingston University, Kingston-upon-Thames, London KT1 2EE, UK.

[c] Department of Pharmaceutical Analytical Chemistry, Faculty of Pharmacy, Assiut University, Assiut, Egypt.

*e-mail: Almontaser_bellah@aun.edu.eg

Fluorescence quantum yields (QYs) of N-CDs/GSH-CuNCs

The QYs of N-CDs and CuNCs were calculated using quinine sulfate (0.1 M H_2SO_4 as solvent) as a standard reference, i.e., at the excitation wavelength of 350 nm, its QY was 56% in 0.1 M H_2SO_4 solution. The fluorescent spectra of quinine sulfate, N-CDs and CuNCs were measured at excitation wavelengths of 350 nm and the absorbance was kept under 0.05. The QYs were determined by plotting the integrated fluorescence intensities against absorbance for the synthesized nanoparticles and quinine sulfate reference standards. The slopes of the linear fits for quinine sulfate, N-CDs, and CuNCs were 99.83, 51.7, and 60.72, respectively. These slope values were used along with the refractive indices and literature QY for quinine sulfate (56%) in the quantitative QY calculations according to the standard equation. The excellent linearity (R^2 > 0.99) of the intensity versus absorbance plots for all three samples provided robust slope values for input into the QY formula to determine accurate fluorescence efficiencies of 29.0 % for N-CDs and 34.0 % for CuNCs. The QYs were calculated according to the following equation:

$$\phi_{Sm} = \phi_{Qs} \times \frac{F_{Sm}}{F_{Qs}} \times \frac{A_{Qs}}{A_{Sm}} \times \frac{\eta_{Sm}}{\eta_{Qs}}$$

where Q denotes the QY of N-CDs or CuNCs; F and A are the integral area of fluorescence emission peak and UV–Vis absorbance intensity at excitation wavelength, respectively; η is the refractive index of the solvent; and the Qs and Sm represent quinine sulfate and the test samples, respectively.

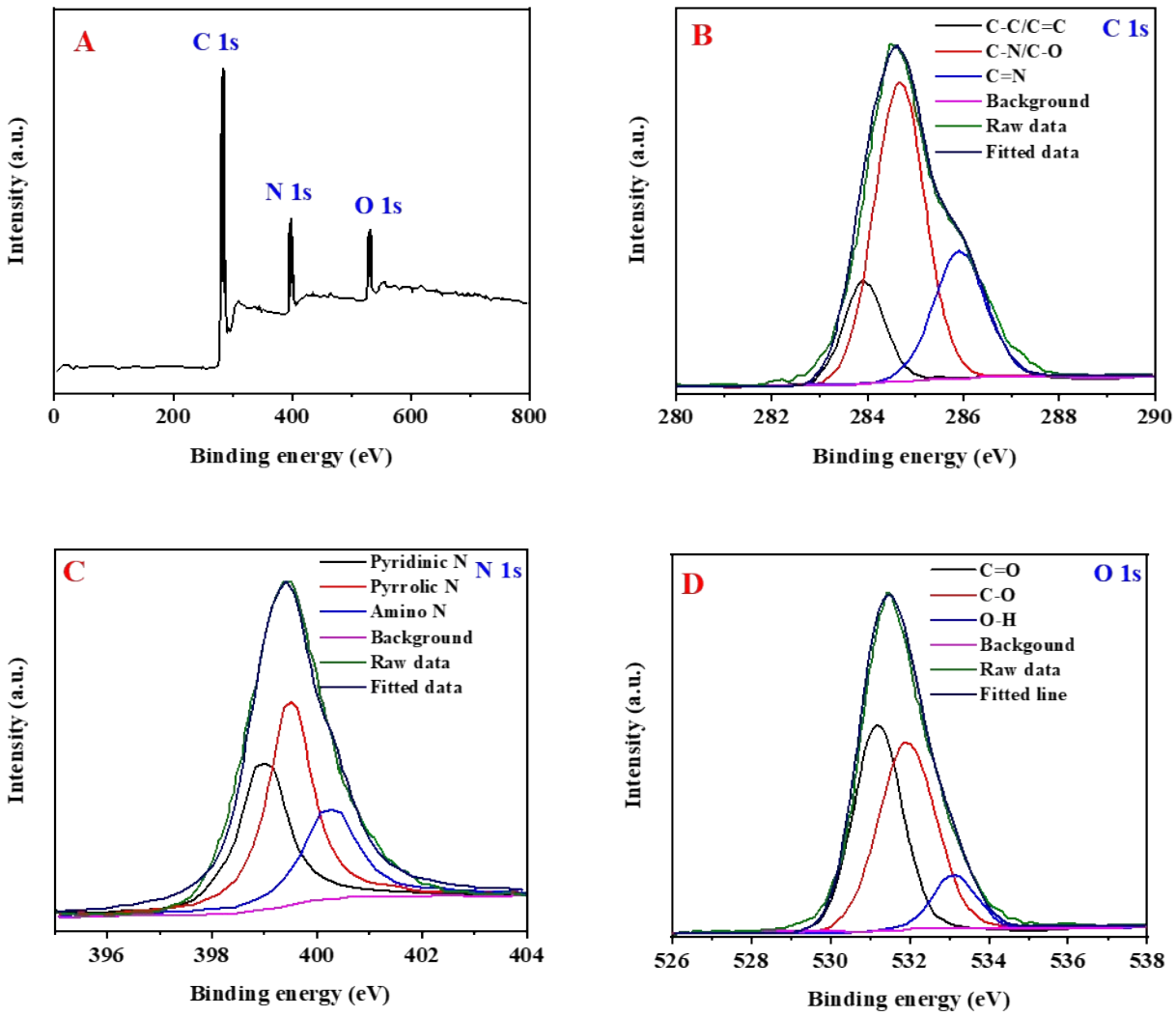

Fig. S1. (A) Raw XPS spectrum of the N-CDs; High-resolution XPS spectra of C 1s (B), N 1s (C), and O 1s (D).

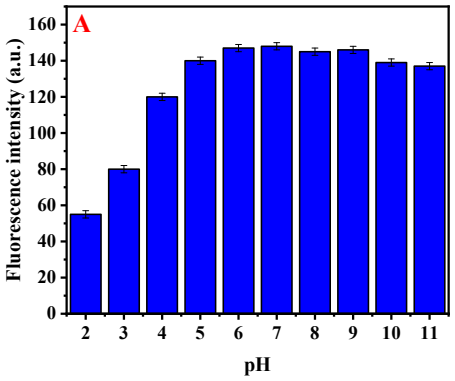
A
Fluorescence intensity (a.u.)
0
20
40
60
80
100
120
140
160
2
3
4
5
6
7
8
9
10
11
pH

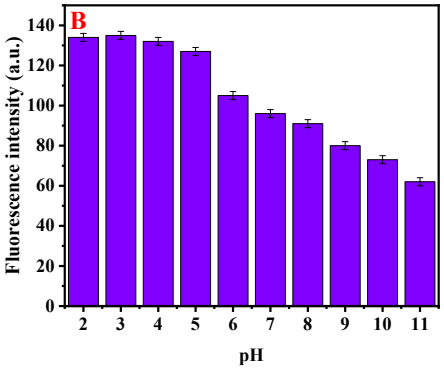
B
Fluorescence intensity (a.u.)
0
20
40
60
80
100
120
140
2
3
4
5
6
7
8
9
10
11
pH

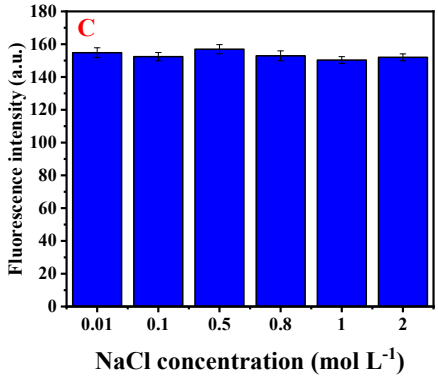
C
Fluorescence intensity (a.u.)
0
20
40
60
80
100
120
140
160
180
0.01
0.1
0.5
0.8
1
2
NaCl concentration (mol L-1)

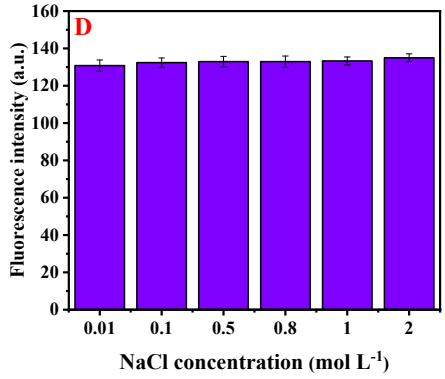
D
Fluorescence intensity (a.u.)
0
20
40
60
80
100
120
140
160
0.01
0.1
0.5
0.8
1
2
NaCl concentration (mol L-1)

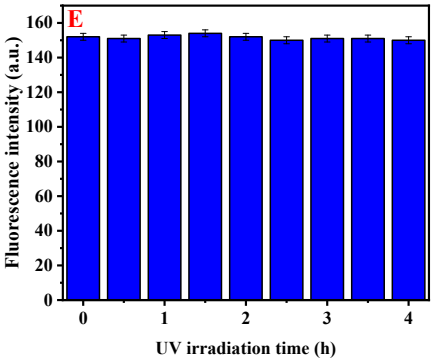
E
Fluorescence intensity (a.u.)
0
20
40
60
80
100
120
140
160
0
1
2
3
4
UV irradiation time (h)

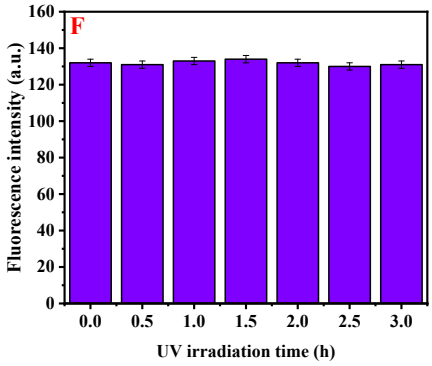
F
Fluorescence intensity (a.u.)
0
20
40
60
80
100
120
140
160
0.0
0.5
1.0
1.5
2.0
2.5
3.0
UV irradiation time (h)

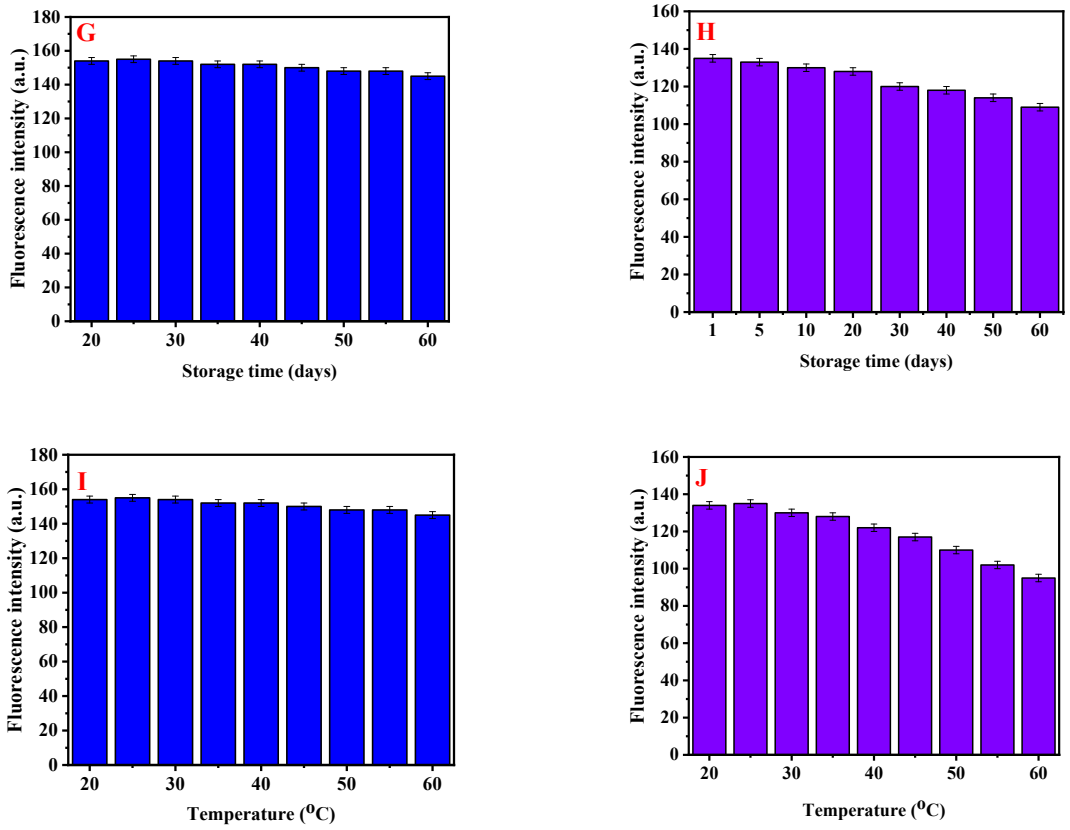

Fig. S2. Stability of the fluorescence response of N-CDs and GSH-CuNCs under various conditions: Effect of pH (2-11) on fluorescence intensity of (A) N-CDs, (B) GSH-CuNCs. Effect of NaCl concentration (0.01-2.0 mol L^{-1}) on fluorescence intensity of (C) N-CDs, (D) GSH-CuNCs. Effect of storage time (0-60 days) on fluorescence intensity of (E) N-CDs, (F) GSH-CuNCs. Effect of UV irradiation time (0-3 hrs) on fluorescence intensity of (G) N-CDs, GSH-CuNCs. Effect of temperature (20-60°C) on fluorescence intensity of (I) N-CDs, (J) GSH-CuNCs.

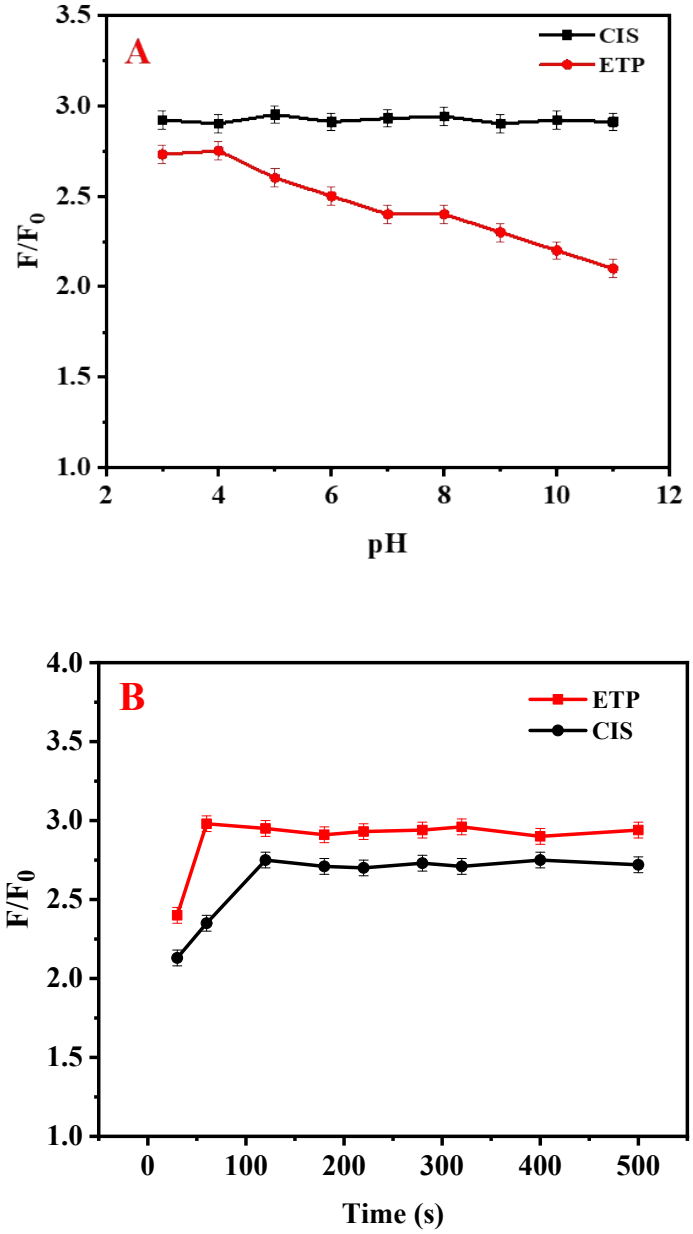

Fig. S3. Influence of (A) pH (3–11) and (B) incubation time (0-500 s) on fluorescence intensity of N-CDs/GSH-CuNCs upon reaction with CIS/ETP.

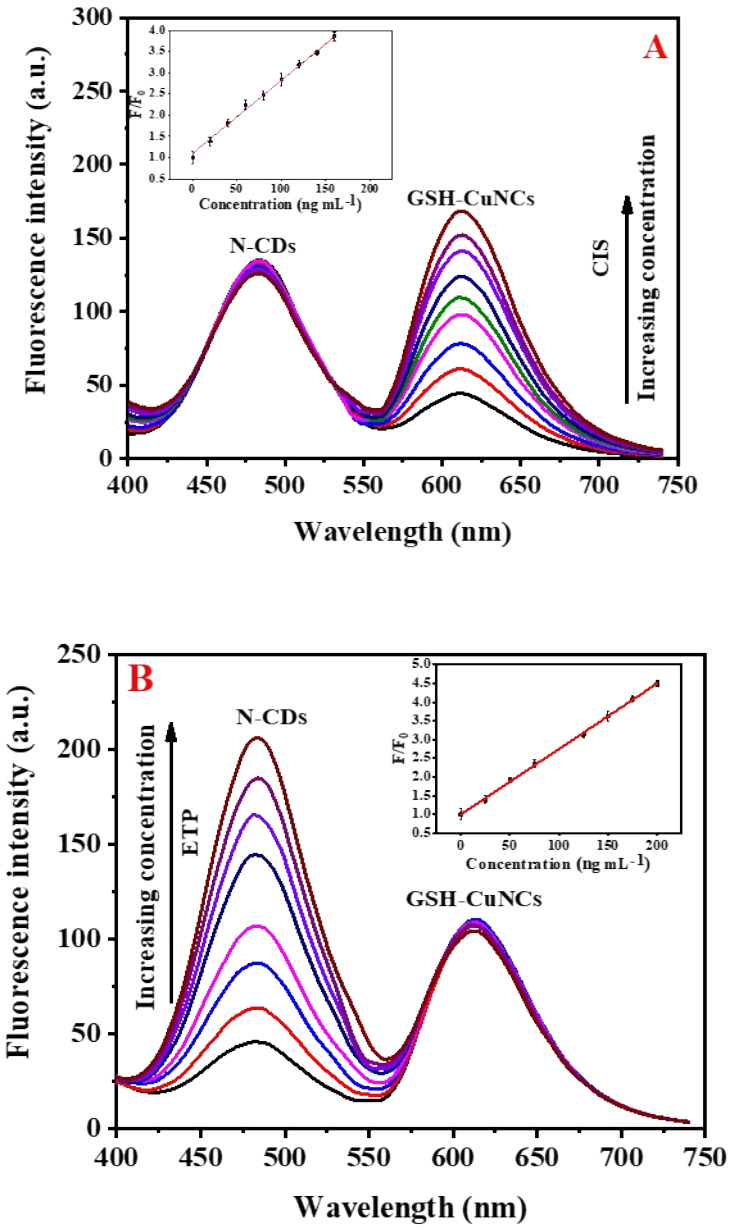

Fig. S4. The influence of different concentrations of (A) CIS (20 – 160 ng mL^{-1}) and (B) ETP (25 – 200 ng mL^{-1}) on the fluorescence emission of N-CDs/GSH-CuNCs.

Table S1: Comparison of this work with other reported fluorescent probes for the detection of CIS

Probe	LOD (ng mL^{-1})	Linear range (µg mL^{-1})	Matrix	Ref.
Rhodamine dithiocarbamate	24	0 – 3.0	Mitochondria	[1]
Rhodamine 640	68	0.6 −15	Cells and zebrafish	[2]
Fluorescent Sensor Array	Not given	0.15 – 1.5	Human Plasma	[3]
G-quadruplex/ Thioflavin T	Not given	0.003 – 0.15	Urine samples	[4]
G-quadruplex DNA-based	216	0.3 – 3.0	Urine samples	[5]
Coumarin-466 /rhodamine-6G	32.7	0 – 48	Intracellular	[6]
N-CDs/GSH-CuNCs	5.2	0.02 – 0.16	Rabbit plasma	**This work**

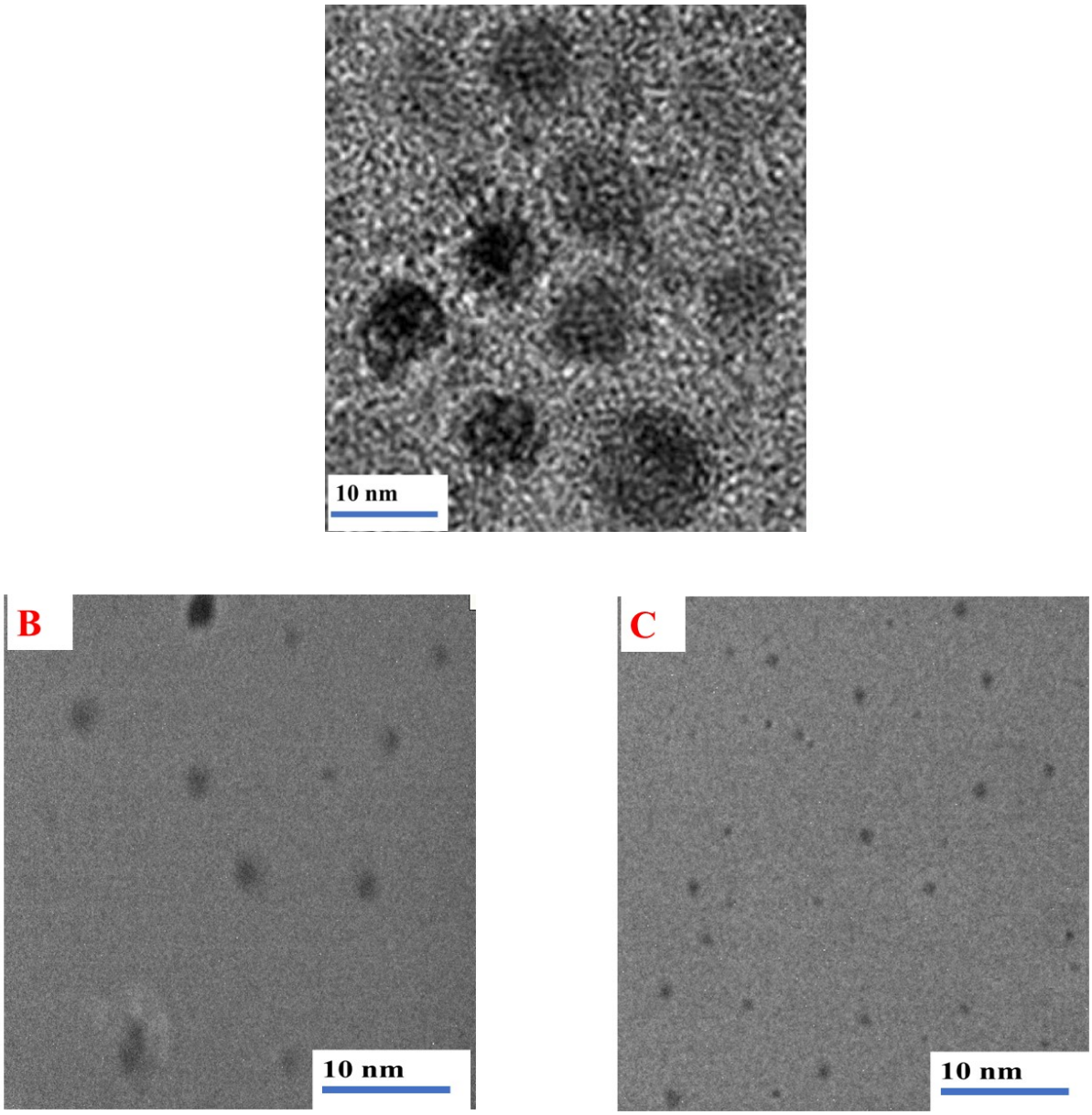

Fig. S5. TEM images of (A) aggregated CuNCs, (B) aggregated N-CDs and (C) disaggregated N-CDs

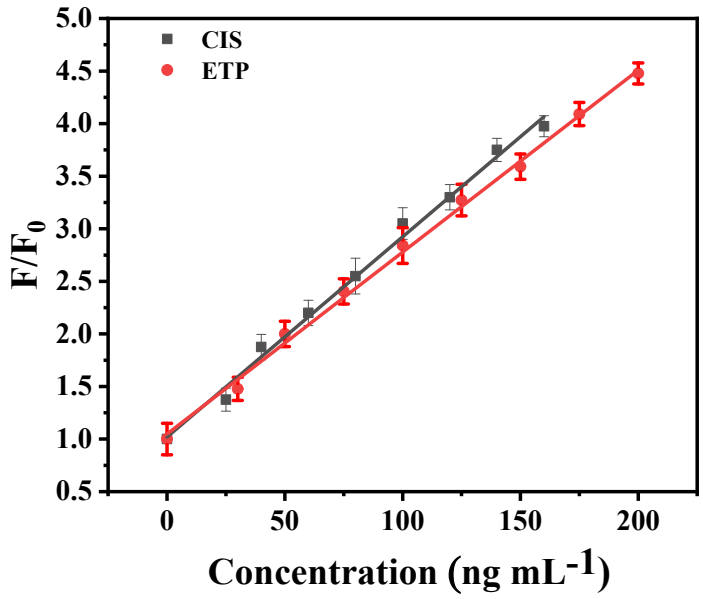

Fig. S6. Plot of (F/F_0) versus concentration of GNT (25 – 160 ng mL^{-1}) and ETP (30 – 200 ng mL^{-1}) in spiked rabbit plasma.

References

[1] J.X. Ong, H.V. Le, V.E.Y. Lee, W.H. Ang, A Cisplatin-Selective Fluorescent Probe for Real-Time Monitoring of Mitochondrial Platinum Accumulation in Living Cells, Angew Chem Int Ed Engl, 60 (2021) 9264-9269.

[2] F. Fan, L. Zhang, F. Mu, G. Shi, Using a High Quantum Yield Fluorescent Probe with Two-Photon Excitation to Detect Cisplatin in Biological Systems, ACS Sensors, 6 (2021) 1400-1406.

[3] L. Mitchell, C. Shen, H.C. Timmins, S.B. Park, E.J. New, A Versatile Fluorescent Sensor Array for Platinum Anticancer Drug Detection in Biological Fluids, ACS Sensors, 6 (2021) 1261-1269.

[4] T. Jantarat, S. Chuaychob, C. Thammakhet-Buranachai, P. Thavarungkul, P. Kanatharana, W. Srisintorn, C. Buranachai, A Label-free DNA-based Fluorescent Sensor for Cisplatin Detection, Sensors and Actuators B: Chemical, 326 (2021) 128764.

[5] H. Yang, H. Cui, L. Wang, L. Yan, Y. Qian, X.E. Zheng, W. Wei, J. Zhao, A label-free G-quadruplex DNA-based fluorescence method for highly sensitive, direct detection of cisplatin, Sensors and Actuators B: Chemical, 202 (2014) 714-720.

[6] J.X. Ong, C.S.Q. Lim, H.V. Le, W.H. Ang, A Ratiometric Fluorescent Probe for Cisplatin: Investigating the Intracellular Reduction of Platinum(IV) Prodrug Complexes, 58 (2019) 164-167.